isvr Institute of Sound and Vibration Research

Coherence Functions for Causally Constrained Systems

S.J. Elliott, J.G. Cook and B. Rafaely

ISVR Technical Memorandum 831

December 1998

University of Southampton

SCIENTIFIC PUBLICATIONS BY THE ISVR

Technical Reports are published to promote timely dissemination of research results by ISVR personnel. This medium permits more detailed presentation than is usually acceptable for scientific journals. Responsibility for both the content and any opinions expressed rests entirely with the author(s).

Technical Memoranda are produced to enable the early or preliminary release of information by ISVR personnel where such release is deemed to the appropriate. Information contained in these memoranda may be incomplete, or form part of a continuing programme; this should be borne in mind when using or quoting from these documents.

Contract Reports are produced to record the results of scientific work carried out for sponsors, under contract. The ISVR treats these reports as confidential to sponsors and does not make them available for general circulation. Individual sponsors may, however, authorize subsequent release of the material.

UNIVERSITY OF SOUTHAMPTON

INSTITUTE OF SOUND AND VIBRATION RESEARCH

SIGNAL PROCESSING & CONTROL GROUP

Coherence Functions for Causally Constrained Systems

by

S J Elliott, J G Cook and B Rafaely

ISVR Technical Memorandum No. 831

December 1998

Authorised for issue by
Prof S J Elliott
Group Chairman

ACKNOWLEDGEMENTS

J G Cook is supported by EPSRC Research Grant GR/L62979. The collaboration of Lotus Engineering in the acquisition of road noise data is also gratefully acknowledged.

CONTENTS

DRAWINGS

1. INTRODUCTION AND DERIVATION

The ordinary coherence function can be used to calculate the ratio of the total power in a signal to the power of that component of the signal which is linearly related to another signal. Consider the model problem shown in Figure 1, in which the observed output signal, $y(t)$, is the sum of that which is linearly related to another signal, $x(t)$, and a "noise" signal, $n(t)$. The noise signal may be composed of measurement noise or components of $y(n)$ which are non-linearly related to $x(t)$. The spectrum of the observed output is thus

$$Y(j\omega) = Z(j\omega) + N(j\omega) , \tag{1}$$

where

$$Z(j\omega) = H(j\omega)X(j\omega) , \tag{2}$$

$H(j\omega)$ is the frequency response of the linear system H in Figure 1, and $X(j\omega)$ and $N(j\omega)$ are the spectra of $x(t)$ and $n(t)$.

The power spectral density of the component of $y(t)$ which is linearly related to $x(t)$ is

$$S_{zz}(j\omega) = |H(j\omega)|^2 S_{xx}(j\omega) \tag{3}$$

where $S_{xx}(j\omega)$ is the power spectral density of $x(t)$. The ratio of $S_{zz}(j\omega)$ to the power spectral density of $y(t)$, $S_{yy}(j\omega)$, is thus

$$\frac{S_{zz}(j\omega)}{S_{yy}(j\omega)} = |H(j\omega)|^2 \frac{S_{xx}(j\omega)}{S_{yy}(j\omega)} . \tag{4}$$

The cross spectral density between $x(t)$ and $y(t)$ is equal to

$$S_{xy}(j\omega) = H(j\omega)S_{xx}(j\omega) \tag{5}$$

so that equation (4), which is equal to the ordinary coherence function between $x(t)$ and $y(t)$, $\gamma_{xy}^2(j\omega)$ [1], is equal to

$$\gamma_{xy}^2(j\omega) = \frac{S_{zz}(j\omega)}{S_{yy}(j\omega)} = \frac{\left|S_{xy}(j\omega)\right|^2}{S_{xx}(j\omega)S_{yy}(j\omega)} . \tag{6}$$

It is important to note that $H(j\omega)$ is not constrained to be causal and so it is impossible to infer a "cause and effect" relationship between $x(t)$ and $y(t)$ from the ordinary coherence function [1]. Indeed the ratio of the total power in $x(t)$ to that which is linearly related to $y(t)$ can be similarly derived to be the coherence function between $y(t)$ and $x(t)$, which is

$$\gamma_{yx}^2(j\omega) = \gamma_{xy}^2(j\omega) \tag{7}$$

since

$$S_{yx}(j\omega) = S_{xy}^*(j\omega) , \tag{8}$$

where * denotes complex conjugation.

If, however, we only consider the component of the signal $y(t)$ which is causally related to $x(t)$, $c(t)$, its power spectral density may be written as

$$S_{cc}(j\omega) = \left|\{H(j\omega)\}_+\right|^2 S_{xx}(j\omega) \tag{9}$$

where the notation $\{\ \}_+$ denotes the Fourier transform of only the causal part of the inverse Fourier transform of the quantity in the brackets, as used in Wiener filtering [2,3]. Explicitly we can write

$$\{H(j\omega)\}_+ \;=\; \mathcal{F}\left[U(t)\,\mathcal{F}^{-1}H(j\omega)\right] \tag{10}$$

where $\mathcal{F}$ denotes the Fourier transform and $U(t)$ is the unit step function which is one for $t \geq 0$ and is otherwise zero. The generation of $c(t)$ is illustrated in Figure 2, in which the "noise" signal, $m(t)$, now contains the components of $y(t)$ which are non-causally related to $x(t)$, as well as those non-linearly related to $x(t)$ and measurement noise.

Taking the measured estimate of the unconstrained frequency response between $x(t)$ and $y(t)$ from equation (5), the ratio of the power spectral density of the component $y(t)$ which is linearly and causally derived from $x(t)$, equation (9), to the power spectral density of $y(t)$ can be written as

$$\frac{S_{cc}(j\omega)}{S_{yy}(j\omega)} \;= {}_c\gamma^2_{xy}(j\omega) \;=\; \frac{S_{xx}(j\omega)}{S_{yy}(j\omega)}\left|\left\{\frac{S_{xy}(j\omega)}{S_{xx}(j\omega)}\right\}_+\right|^2 \tag{11}$$

which may be termed the *causal coherence function* between x and y.

Notice that generally

$${}_c\gamma^2_{xy}(j\omega) \;\neq {}_c\gamma^2_{yx}(j\omega) \tag{12}$$

and that although

$$\int_o^\infty \left|\{H(j\omega)\}_+\right|^2 d\omega \;\leq\; \int_o^\infty |H(j\omega)|^2\, d\omega \tag{13}$$

$\left|\{H(j\omega)\}_+\right|^2$ is not necessarily less than $|H(j\omega)|^2$ at each frequency and so ${}_c\gamma^2_{xy}(j\omega)$ is not necessarily less than $\gamma^2_{xy}(j\omega)$ at each ω, although this will be true when averaged across frequencies.

Although $c(t)$ in Figure 2 is derived from a causal filtering of $x(t)$, which is equal to the causal part of the estimated frequency response given by solving equation (5), this is not the optimum least squares estimate of $y(t)$ which can be derived from $x(t)$. This optimum least squares estimate would minimise the difference between the output of the filter and $y(t)$, and could use the predictability of $x(t)$ to achieve this. The frequency response of this optimum causal filter was derived by Wiener [2, see also 3] and can be written as

$$H_w(j\omega) = \frac{1}{F(j\omega)} \left\{ \frac{S_{xy}(j\omega)}{F^*(j\omega)} \right\}_+ \tag{14}$$

where $F(j\omega)$ is the causal, minimum phase spectral factor of $S_{xx}(j\omega)$, so that

$$S_{xx}(j\omega) = F(j\omega)\, F^*(j\omega) \tag{15}$$

and $\{\ \}_+$ denotes the Fourier transform of the causal part of the inverse Fourier transform of the quantity in brackets, as above. The block diagram for such a system is shown in Figure 3, in which the mean square value of the "noise" signal, $l(t)$, is now minimised by causally filtering $x(t)$ to produce $p(t)$. The ratio of the power spectral density of $p(t)$ to that of $y(t)$ can thus be written, using equation (4), (14) and (15) as

$$\frac{S_{pp}(j\omega)}{S_{yy}(j\omega)} = {}_p\gamma^2_{xy}(j\omega) = \frac{1}{S_{yy}(j\omega)} \left| \left\{ \frac{S_{xy}(j\omega)}{F^*(j\omega)} \right\}_+ \right|^2 \tag{16}$$

which may be termed the *predictive coherence function.* Generally speaking this will be greater than the causal coherence function, because the predictability of $x(t)$ has been used in its derivation.

2. PRACTICAL CALCULATION

The causal coherence function may be calculated in practice from sampled stationary random data by first computing the discrete frequency version of the power spectral densities of $x(t)$ and $y(t)$, and their cross spectral density, by averaging over the FFTs of consecutive blocks of data in the usual way [1].

The ordinary coherence function can then be calculated as

$$\gamma_{xy}^2(k) = \frac{\left|S_{xy}(k)\right|^2}{S_{xx}(k)S_{yy}(k)} \tag{17}$$

where k is the discrete frequency variable corresponding to the true frequency of kf_s/N where f_s is the sample rate and N is the number of data points in the FFT. The usual care must be taken to ensure that the circular effects of the FFT and the sidelobes of the time window do not unduly affect the accuracy of the estimated spectral densities [1].

The discrete frequency response of the linear system in Figure 1 is given by

$$H(k) = \frac{S_{xy}(k)}{S_{xx}(k)} . \tag{18}$$

Taking the inverse FFT of this frequency response allows the noncausal part, from $n = N/2$ to $N-1$, to be set to zero and thus calculate

$$\{H(k)\}_+ = FFT\left[U(n)\,IFFT(H(k))\right] \tag{19}$$

where $U(n) = 1$ from $n = 0$ to $N/2-1$ and is otherwise zero. It is assumed that the size of the FFT, N, is large enough that the causal part of the IFFT of $H(k)$ is not affected by the circular

effects from its noncausal parts. The discrete frequency version of the causal coherence function is then

$$ {}_c\gamma^2_{xy}(k) \;=\; \frac{S_{xx}(k)}{S_{yy}(k)}\left|\{H(k)\}_+\right|^2 . \tag{20} $$

In order to calculate the predictive coherence function the spectral factors of $S_{xx}(k)$ may first be obtained by calculating the minimum phase component of the system whose frequency response has a modulus of $\left(S_{xx}(k)\right)^{\frac{1}{2}}$. This can conveniently be achieved using the cepstral method of calculating the discrete Hilbert transform [4], so that

$$ F(k) \;=\; \exp\left[FFT\left(c(n)\,IFFT\left[\log_e\left(S_{xx}(k)\right)\right]\right)\right] \tag{21} $$

where $c(n)$ is equal to $\frac{1}{2}$ for $n > 0$, is equal to 0 for $n < 0$ and is equal to $\frac{1}{4}$ for $n = 0$. The causality operation $\{\ \}_+$, can be easily calculated for discrete data, as above. Some care must again be taken to ensure that the size of the FFT used, N, is sufficient for its circular nature not to interfere with the causality operation. This is illustrated in Figure 4, in which the continuous spectrum of an example of the function $S_{xd}\left(e^{j\omega T}\right)/F^*\left(e^{j\omega T}\right)$ is plotted for sampled data in Figure 4(a), together with its inverse Fourier transform in Figure 4(c). The time domain response in Figure 4(c) lasts about 20 samples in this case. The FFT size must be at least twice as long as this, and Figure 4(b) shows the discrete frequency spectrum $S_{xd}(k)/F(k)$ for an FFT size of 64 points. The causal part of the inverse FFT of this spectrum, Figure 4(d), extends from sample 0 to sample 31, and clearly is a faithful representation of the true response, shown in Figure 4(c), over this range of samples.

Once the spectral factors of $S_{xx}(k)$ has been calculated, together with the causal part of $S_{xd}(k)/F^*(k)$, the predictive coherence function can be calculated at the discrete frequency k as

$$ {}_p\gamma^2_{xy}(k) \;=\; \frac{1}{S_{yy}(k)}\left|\left\{\frac{S_{xy}(k)}{F^*(k)}\right\}_+\right|^2 \tag{22} $$

3. EXAMPLE CALCULATIONS

In this section several example calculations will be presented to illustrate the properties of the causal and predictive coherence, first on synthetic signals and then on measured signals.

In the first example a random signal with a 3dB/octave spectrum (pink noise) was used as the input signal $x(n)$. The output signal was equal to a sum of this signal weighted by a factor of $\frac{1}{2}$ and delayed by one sample and another uncorrelated random pink noise signal of equal variance also weighted by a factor of $\frac{1}{2}$. The magnitude of the frequency response estimate $S_{xy}(k)/S_{xx}(k)$ and its Fourier transform are shown in Figure 5. The FFT block size was 512 samples at an assumed sample rate of 2.5 kHz and the spectral densities were calculated by averaging over 512 blocks of data. The impulse response clearly shows the one sample delay and weighting of 0.5, and since it is substantially zero for the noncausal part of the time window, the Fourier transform of the causal part, also shown in the upper graph in Figure 5, is substantially the same as the original frequency response.

The "forward" causal coherence function, ${}_c\gamma^2_{xy}(k)$, as plotted as the dashed line in Figure 6, is thus very similar to the ordinary coherence function, which as expected is equal to about 0.5 for all frequencies in this example. The "backwards" causal coherence function, ${}_c\gamma^2_{yx}(k)$, however, is almost zero in this case.

The "forward" predictive coherence function, ${}_p\gamma^2_{xy}(k)$, is plotted as the dashed line in Figure 7 and is again similar to the ordinary coherence function, since it is not necessary to use the predictability of $x(t)$ to minimise the mean square difference between the filter output and $y(t)$. The "backwards" predictive coherence function ${}_p\gamma^2_{yx}(k)$ as shown by the dash-dotted line in Figure 7 is now about 0.2, or greater at low frequencies, since the predictability

of the pink noise signal is being used to overcome the inherent one sample advance of the signal $x(t)$ compared with the signal $y(t)$ in this case.

Data was also simultaneously acquired from an accelerometer mounted on the body of a car, $x(t)$, and an internal pressure microphone, $y(t)$, as the car was driven over a coarse road surface. The power spectral densities of the two signals are shown in Figure 8 calculated with an FFT size of 512 samples at a sample rate of 2.5 kHz over 512 blocks of data. The frequency response calculated from $S_{xy}(k)/S_{xx}(k)$ is plotted in Figure 9 together with the corresponding impulse response. The FFT of the causal part of the impulse response is shown as the dashed line in the upper graph in Figure 9. The ordinary coherence function and the causal coherence function, from the acceleration to the pressure, was calculated using the method outlined above and these functions are shown in Figure 10. It can be seen that the causal coherence function is similar to the ordinary coherence function over most of the frequency range plotted in this figure, indicating that most of the part of the pressure signal which is coherent with the accelerometer could be generated by causally filtering the accelerometer signal.

The backwards causal coherence, from microphone to accelerometer, can be calculated from the estimated frequency response between $y(t)$ and $x(t)$, which is equal to $S_{yx}(k)/S_{yy}(k)$. This frequency response and the corresponding impulse response are shown in Figure 11. The estimated response from $y(t)$ to $x(t)$ will, however, be corrupted by any uncorrelated noise in $y(t)$, as shown as $n(t)$ in Figure 1, so that

$$\frac{S_{yx}}{S_{yy}} = \frac{H^* S_{xx}}{|H|^2 S_{xx} + S_{nn}} \tag{23}$$

In this example, where the ordinary coherence function is significantly below unity, S_{nn} is large compared with $|H|^2 S_{xx}$. The backwards causal coherence for the road noise example is shown in Figure 12, and is significantly smaller than the forwards causal coherence function,

which is to be expected, except at very low frequencies for which $S_{yy}(k)/S_{xx}(k)$ is particularly large.

The forward and backward predictive coherence functions are plotted in Figure 13. Although it is to be expected that the forward predictive component is greater than the ordinary coherence at some frequencies, the calculation also suffers from ill conditioning because of the very low values of S_{yy} at high frequencies, whose reciprocal is used to calculate the predictive coherence as in equation (16). The backwards predictive coherence is however small compared with the ordinary coherence except when the ill conditioning occurs at high frequencies.

4. MULTICHANNEL EXTENSIONS

If the spectral density matrix for the input signals of a multiple input single output (MISO) system are defined to be

$$\mathbf{S}_{xx} = E\left[\mathbf{x}(j\omega)\mathbf{x}^H(j\omega)\right] \tag{24}$$

where

$$\mathbf{x}(j\omega) = \left[X_1(j\omega)X_2(j\omega)\cdots X_k(j\omega)\right]^{\mathrm{T}} \tag{25}$$

and the row vector of cross spectral densities is defined as

$$\mathbf{S}_{xy} = E\left[y(j\omega)\mathbf{x}^H(j\omega)\right], \tag{26}$$

then the row vector of frequency responses between $\mathbf{x}$ and y can be written as

$$\mathbf{H}(j\omega) = \mathbf{S}_{xy}\mathbf{S}_{xx}^{-1}. \tag{27}$$

The power spectral density of the sum of the outputs of these filters is

$$S_{zz} = \mathbf{H}\,\mathbf{S}_{xx}\,\mathbf{H}^{H} \tag{28}$$

and so the ratio of this to S_{yy} is

$$\gamma^2_{xy} = \frac{S_{zz}}{S_{yy}} = \frac{\mathbf{S}_{xy}\,\mathbf{S}_{xx}^{-1}\,\mathbf{S}_{xy}^{H}}{S_{yy}}\,, \tag{29}$$

which is the multiple coherence function. Defining the causal parts of the frequency responses derived above to be

$$\{\mathbf{H}\}_{+} = \left\{\mathbf{S}_{xy}\,\mathbf{S}_{xx}^{-1}\right\}_{+} \tag{30}$$

then the MISO extension of the causal coherence can be written as

$${}_{c}\gamma^2_{xy} = \frac{\left\{\mathbf{S}_{xy}\,\mathbf{S}_{xx}^{-1}\right\}_{+}\mathbf{S}_{xx}\left\{\mathbf{S}_{xy}\,\mathbf{S}_{xx}^{-1}\right\}_{+}^{H}}{S_{yy}}\,. \tag{31}$$

The row vector of optimal Wiener filters can also be written as

$$\mathbf{H}_{\text{opt}} = \left\{\mathbf{S}_{xy}\,\mathbf{F}^{-H}\right\}_{+}\mathbf{F}^{-1} \tag{32}$$

where

$$\mathbf{S}_{xx} = \mathbf{F}\,\mathbf{F}^{H} \tag{33}$$

and $\mathbf{F}$ is the matrix of causal minimum phase spectral factors of $\mathbf{S}_{xx}$, so that

$$\mathbf{F}^{-1}\,\mathbf{S}_{xx}\,\mathbf{F}^{-H} = \mathbf{I}. \tag{34}$$

The MISO extension to the predictive coherence function can thus be written as

$$ {}_p\gamma^2_{xy} = \frac{\left\{\mathbf{S}_{xy}\mathbf{F}^{-H}\right\}_+ \left\{\mathbf{S}_{xy}\mathbf{F}^{-H}\right\}_+^H}{S_{yy}} . \qquad (35) $$

5. CONCLUSIONS

A special form of the coherence function is presented which quantifies the degree to which one signal can be causally derived from another. This function is termed the causal coherence. It is shown how this function can be calculated for stationary random sampled data by calculating the power spectral densities and cross spectral density in the usual way, and then using the causal part of the Fourier transform of the frequency response estimated by dividing the cross spectral density by the power spectral density. Example calculations are presented for synthetic pink noise data and for body acceleration and internal pressure data recorded from a car travelling over a rough road. The causal coherence from the acceleration to the pressure is similar to the ordinary coherence, but the causal coherence calculated from the pressure to the acceleration is low, which suggests that the pressure is causally dependant on the acceleration, as expected. Another coherence function can be calculated from the optimum Wiener filter which minimises the difference between the output of a causally filtered version of one signal and the other signal. Since this can use the predictability of the input signal as well as the causal part of the frequency response it is termed the predictive coherence function.

Neither of these new coherence functions are guaranteed to be less than the ordinary coherence function, or indeed less than unity, at any one frequency, although the frequency averaged value of the causal coherence function must be less than that of the ordinary coherence function. Although these extensions to the ordinary coherence functions appear to

give physically meaningful results for the examples discussed in this report, their mathematical and numerical properties are not as obvious as those of the ordinary coherence function and some care needs to be taken in their interpretation.

REFERENCES

1. J.S.BENDAT and A.G.PIERSOL 1986 *Random Data.* New York: John Wiley & Sons, second edition.
2. N.WIENER 1949 *Extrapolation Interpolation and Smoothing of Stationary Time Series.* New York: John Wiley & Sons.
3. T.KAILATH 1981 *Lectures on Wiener and Kulman Filtering.* New York: Springer-Wien.
4. A.V.OPPENHEIM and R.W.SHAFFER 1975 *Digital Signal Processing.* Prentice Hall.

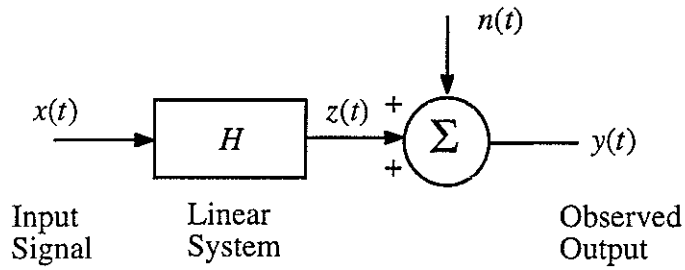

Figure 1 Model problem for the calculation of the ordinary coherence function.

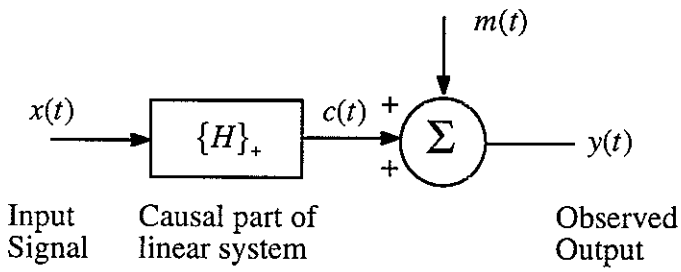

Figure 2 Block diagram for the calculation of the causal coherence function.

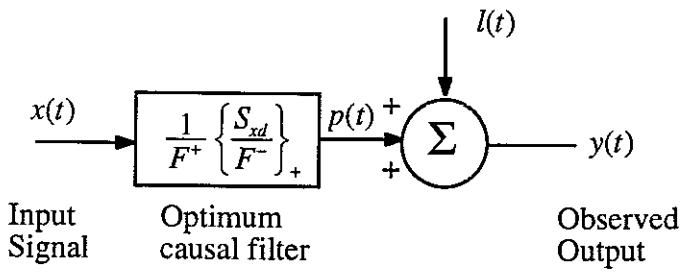

Figure 3 Block diagram for the calculation of the predictive coherence function.

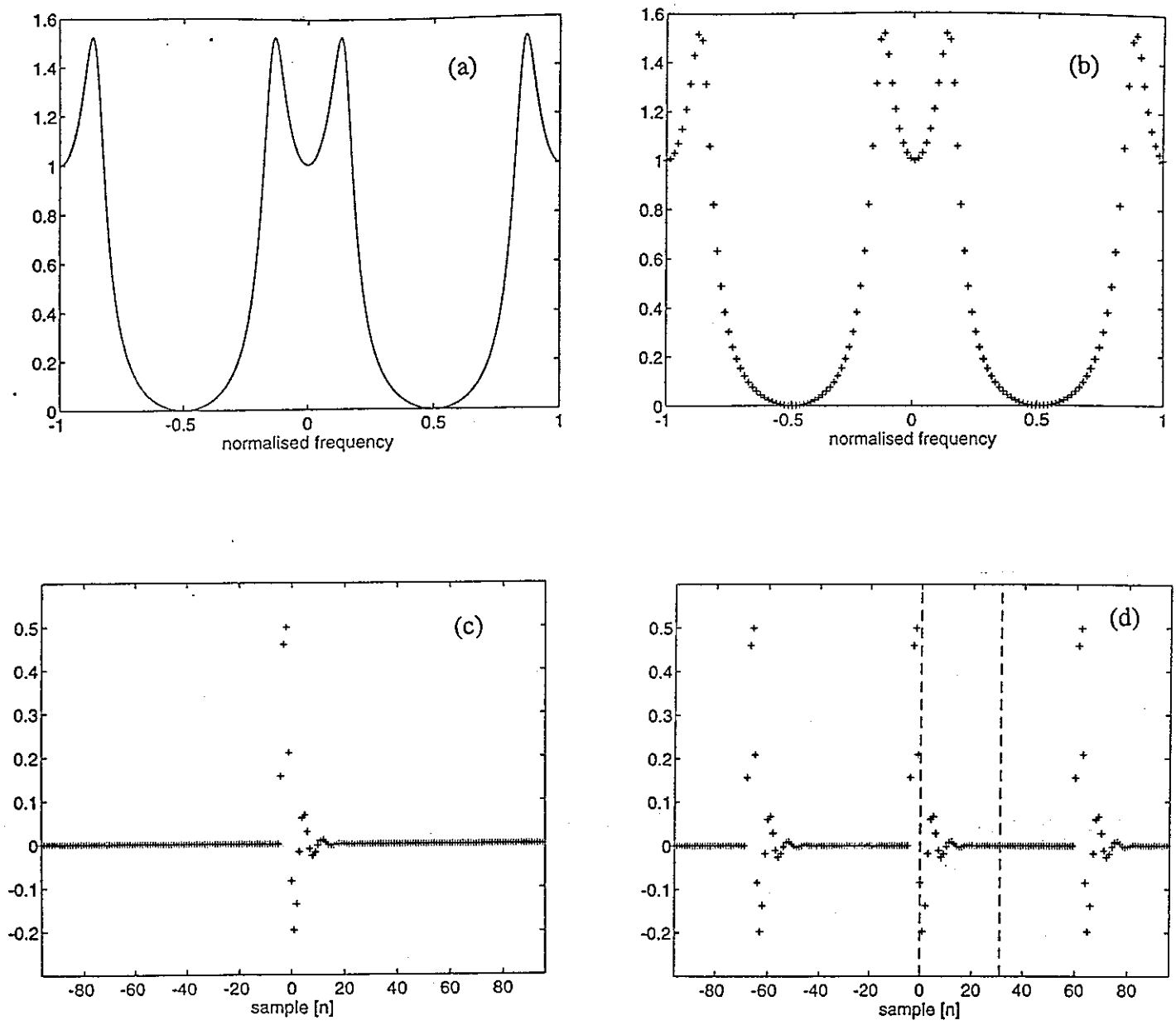

Figure 4 The magnitude of the continuous frequency domain version of $A(e^{j\omega T}) = S_{xd}(e^{j\omega T})/F^*(e^{j\omega T})$, *Fig.4(a), together with its discrete frequency domain version A(k), Fig.4(b), for an example in which this function has a resonant structure and for a FFT size of 64 points. The Wiener filter calculated using the FFT, equation (22), will be accurate providing the inverse Fourier transform of A(k), shown in Fig.4(d), is equal to the inverse Fourier transform of* $A(e^{j\omega T})$, *Fig.4(c) for n = 0 to 32, as shown by the dashed lines in Fig.4(d).*

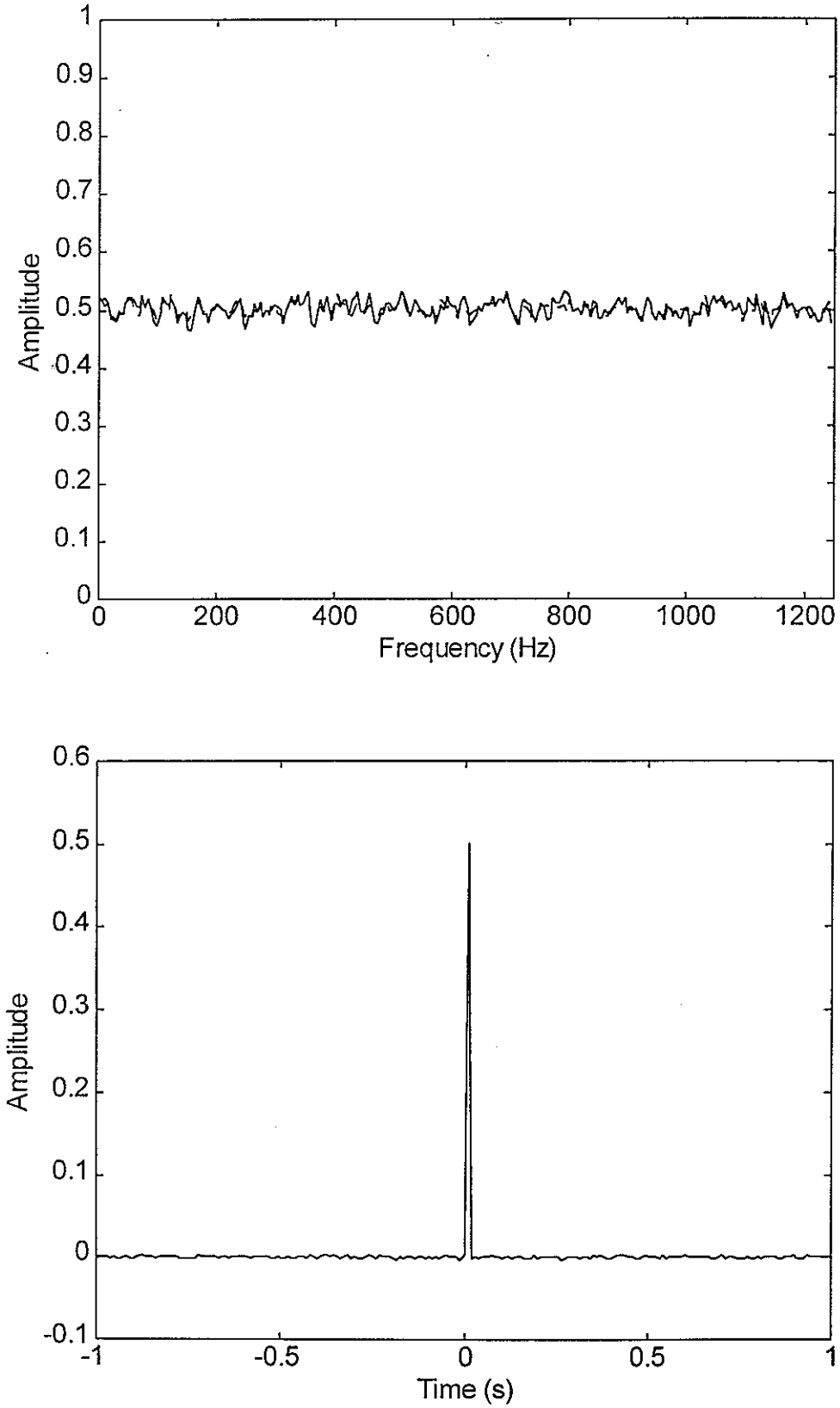

Figure 5 *The frequency response estimate $H(k) = S_{xy}(k)/S_{xx}(k)$ for the synthetic pink noise example (solid line, (upper graph)) and its IFFT (lower graph). The FFT of the causal part of the impulse response, $\{H(k)\}_+$, is also shown as the dashed line in the upper graph.*

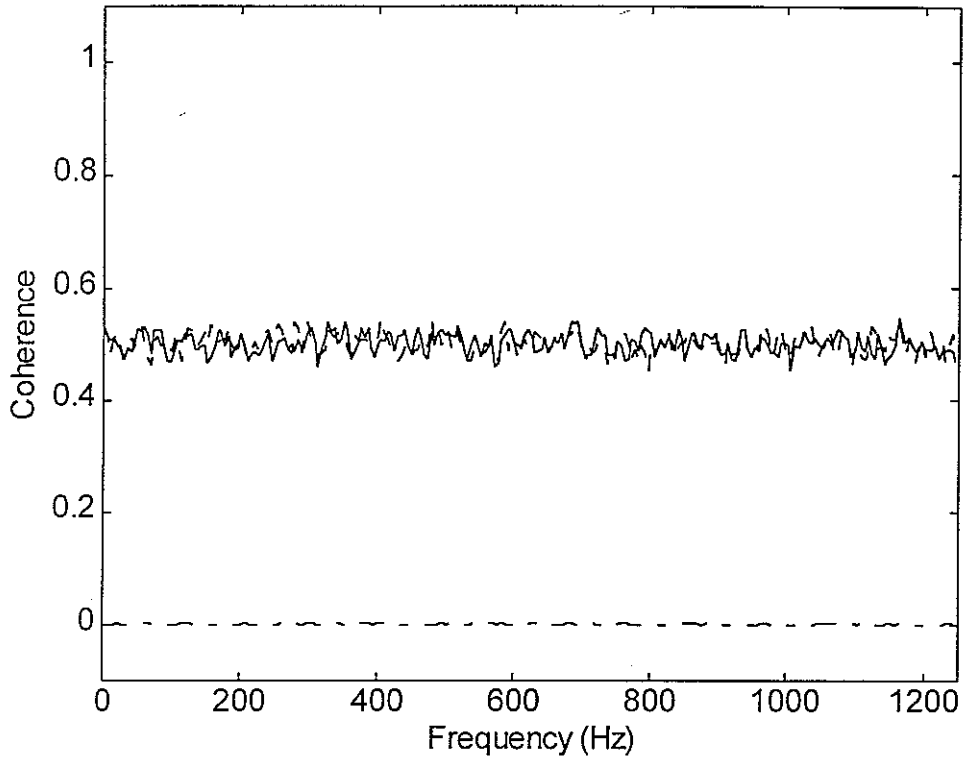

Figure 6 The ordinary coherence for the synthetic pink noise example, $\gamma^2_{xy}(k)$ (solid line), the forward causal coherence, ${}_c\gamma^2_{xy}(k)$ (dashed line) and the backwards causal coherence ${}_c\gamma^2_{yx}(k)$ (dot-dashed line, which is almost zero).

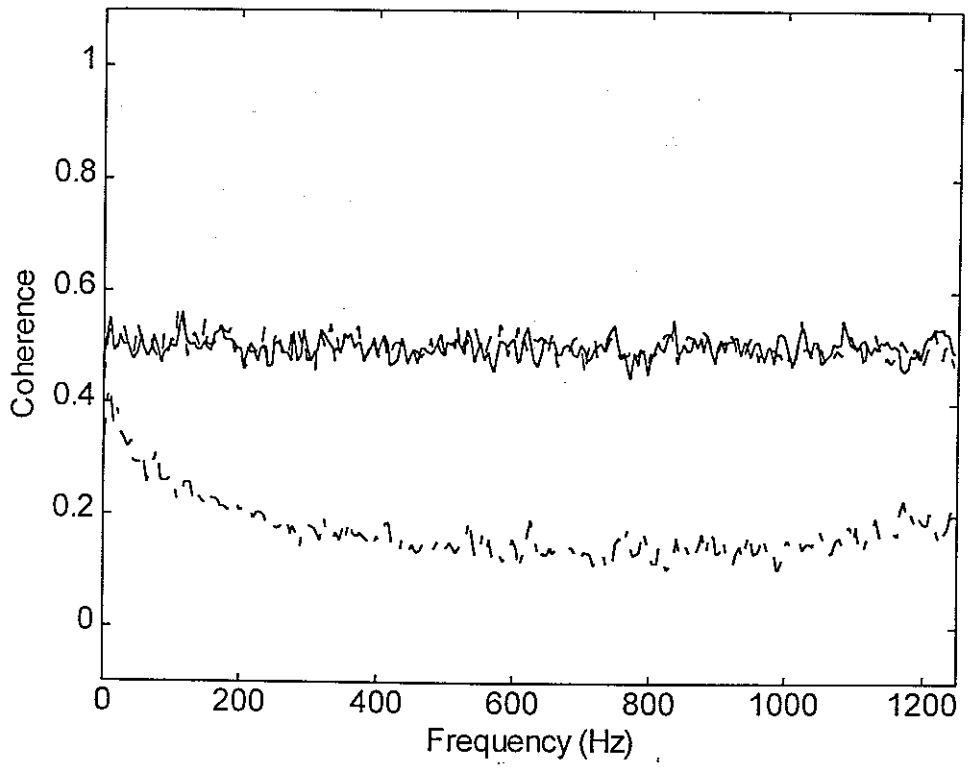

Figure 7 The ordinary coherence function for the synthetic pink noise example $\gamma^2_{xy}(k)$ (solid line), the forward predictive coherence ${}_p\gamma^2_{xy}(k)$ (dashed line) and the backwards predictive coherence ${}_p\gamma^2_{yx}(k)$ (dot-dashed line).

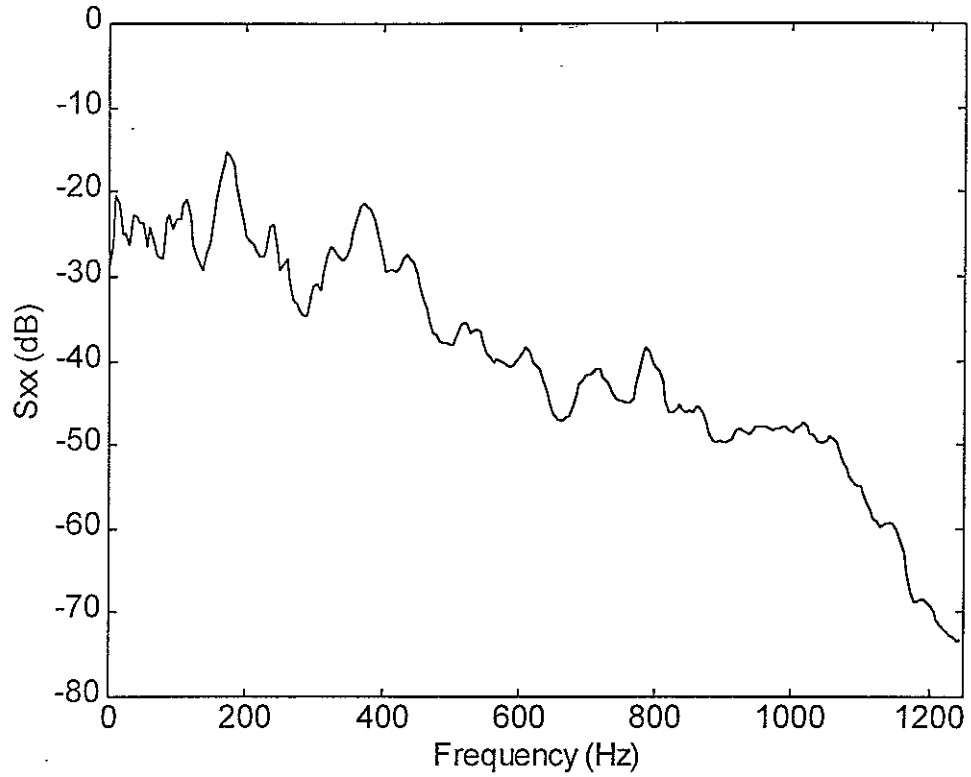

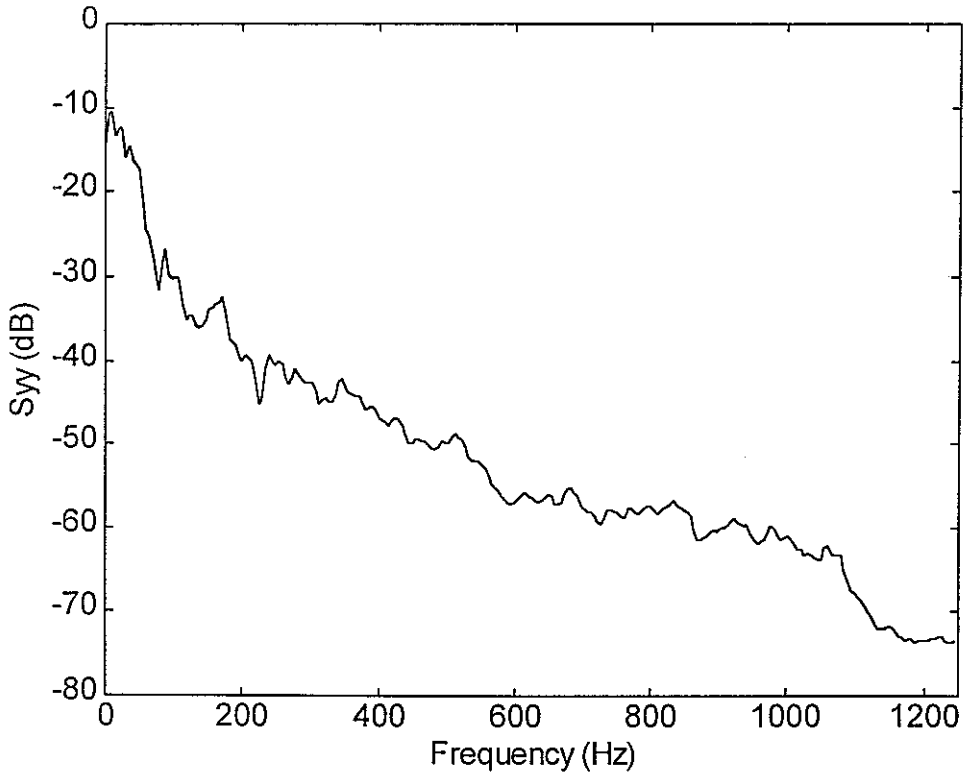

Figure 8 Power spectral density of the accelerometer signal, $S_{xx}(k)$, and microphone signal, $S_{yy}(k)$, measured from the vehicle road noise data.

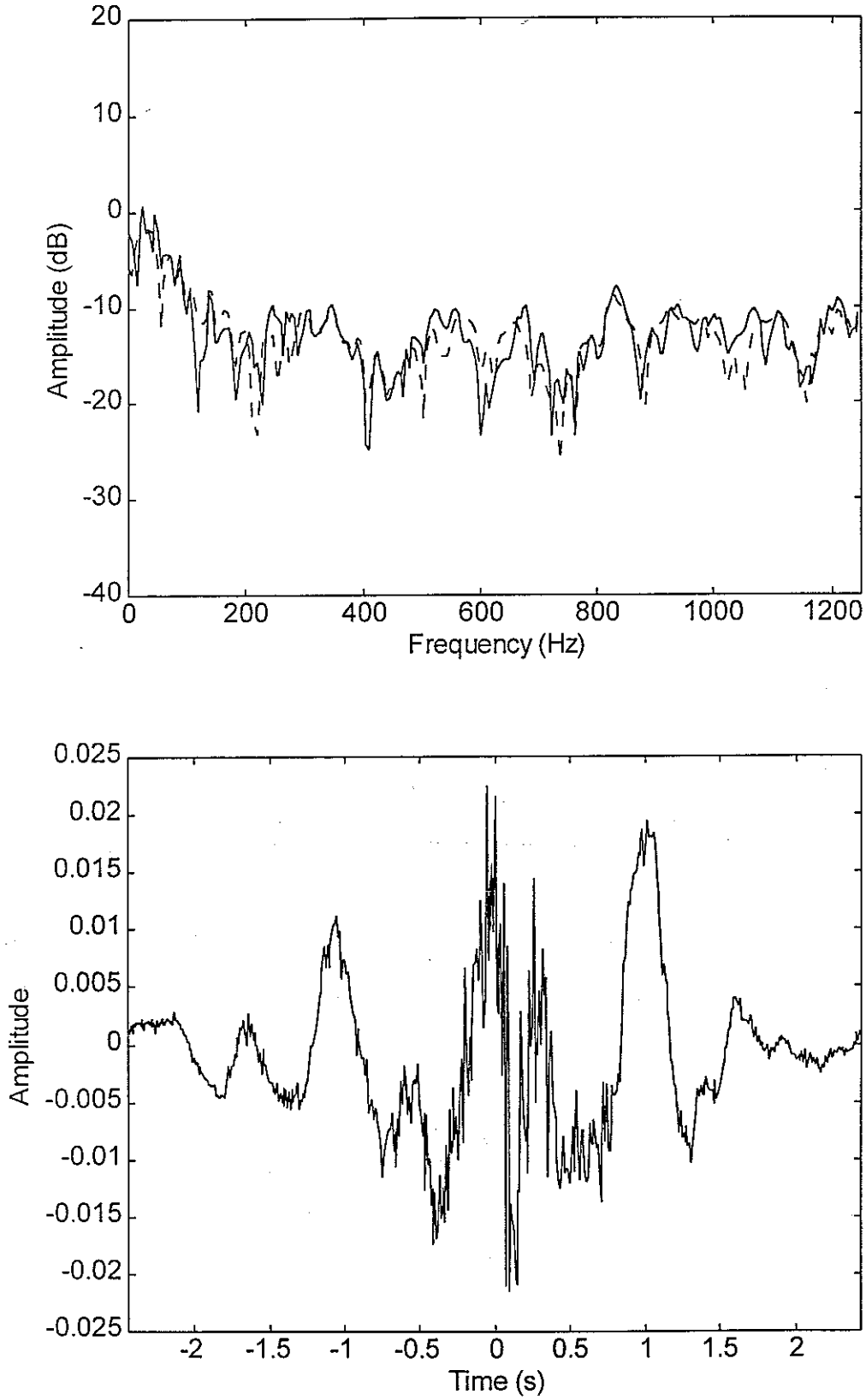

Figure 9 The estimated frequency response from x to y calculated from S_{xy}/S_{xx} together with its causal component, and the corresponding impulse response for the road noise example.

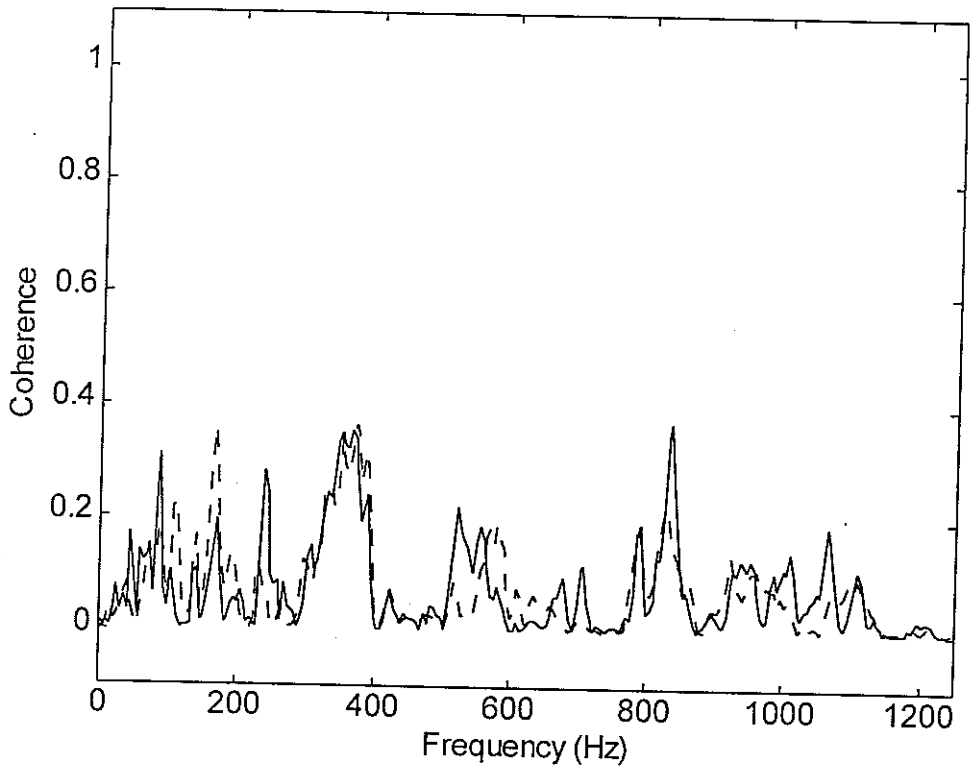

Figure 10 *The ordinary coherence function, γ_{xy}^2 and the forward causal coherence function ${}_c\gamma_{xy}^2$ for the road noise example.*

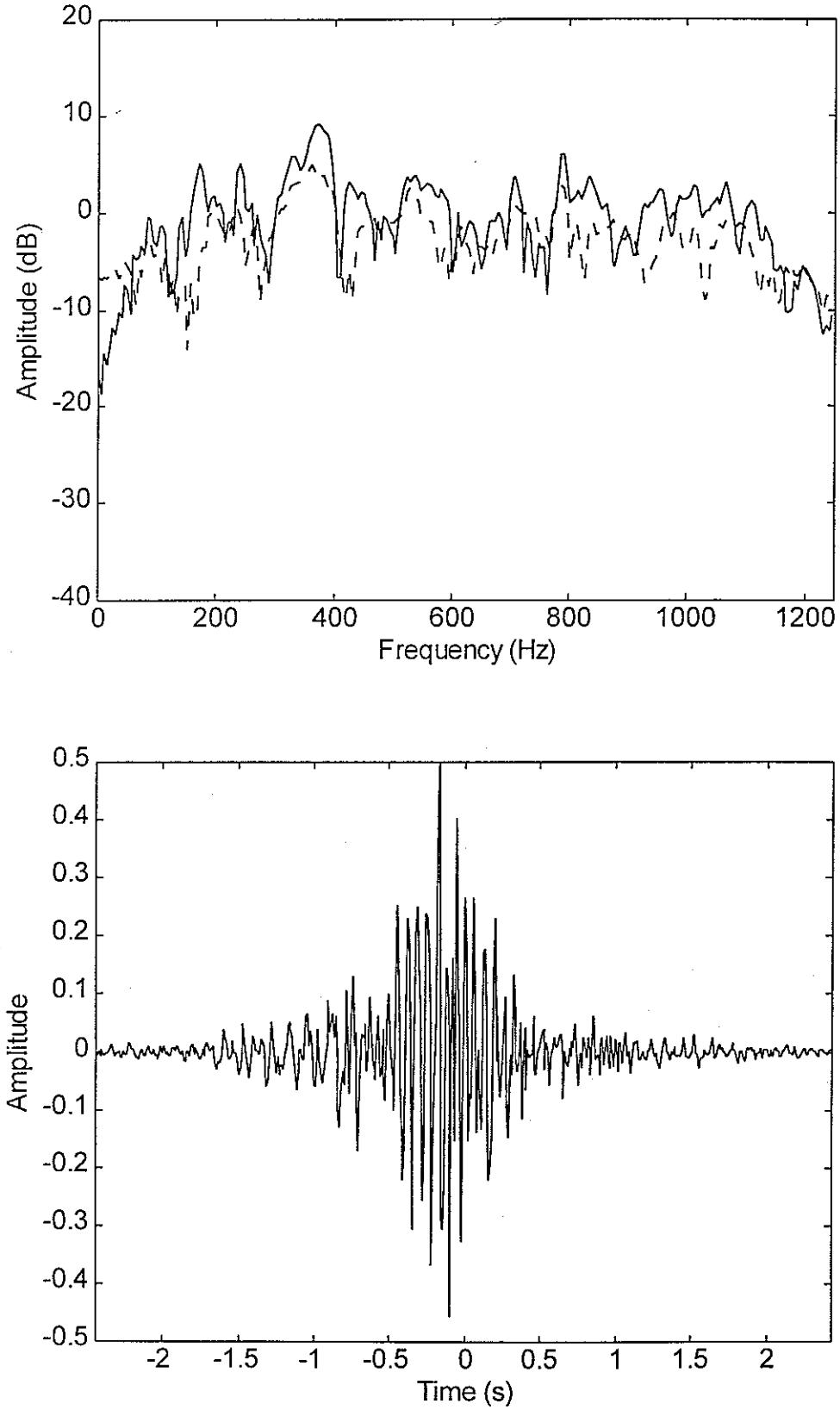

Figure 11 *The estimated frequency response from y to x, calculated from $S_{yx}(k)/S_{yy}(k)$, and the corresponding impulse response, for the road noise example.*

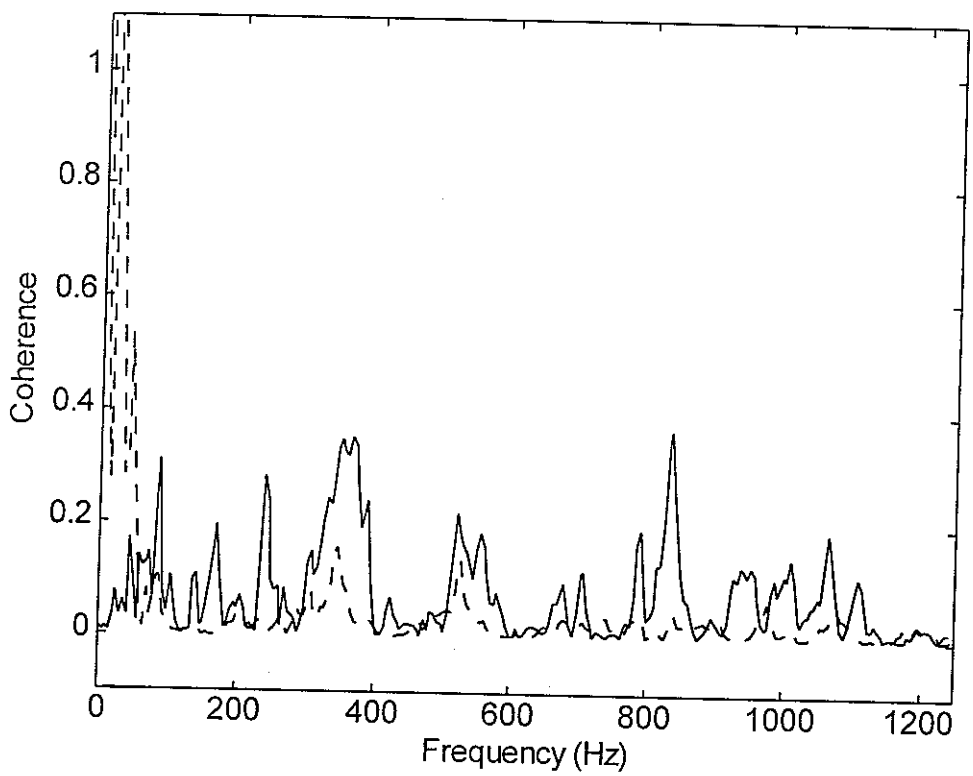

Figure 12 *The ordinary coherence function, γ^2_{xy}, and the backward causal coherence, ${}_c\gamma^2_{yx}$, for the road noise data.*

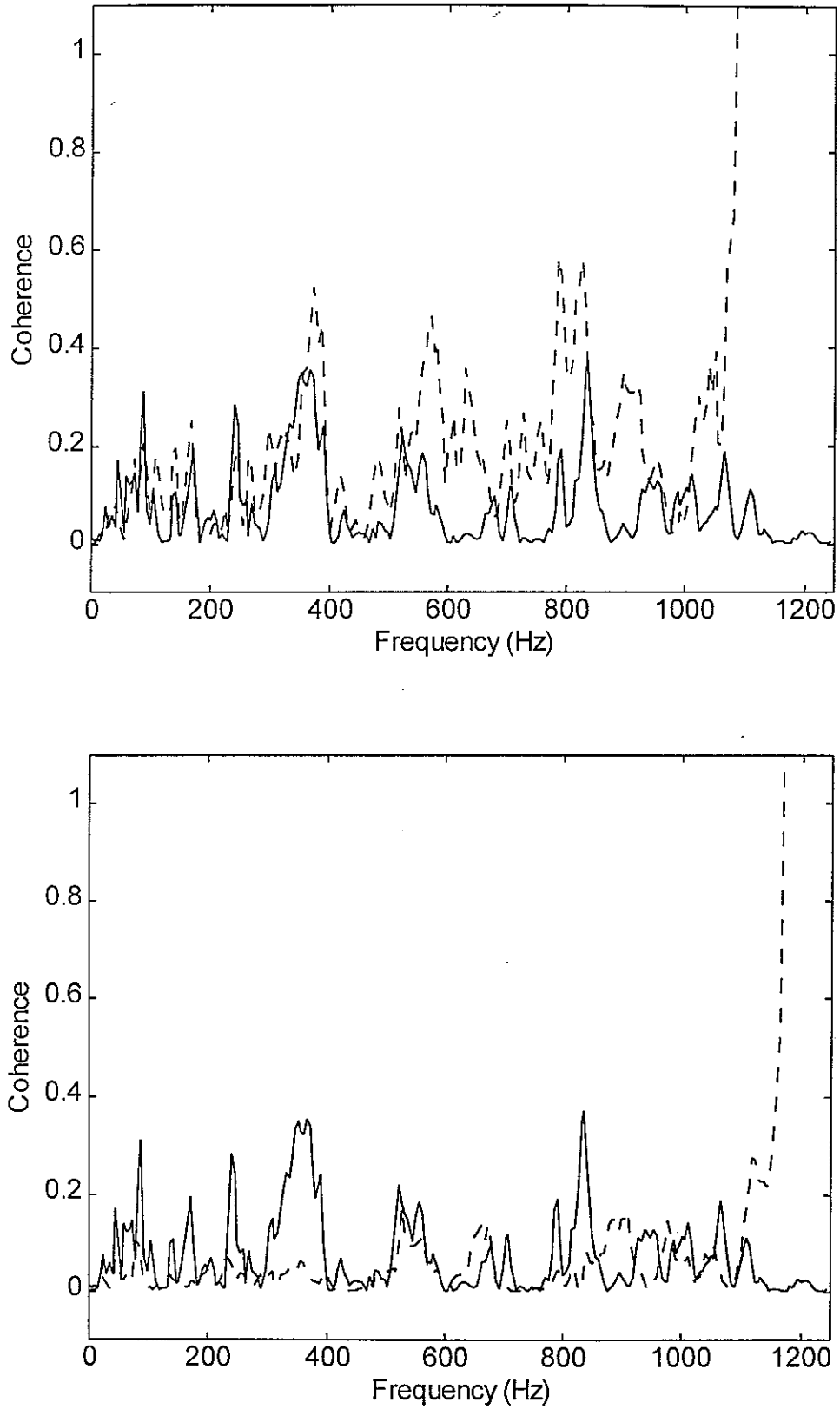

Figure 13 *The forward predictive coherence function, ${}_p\gamma^2_{xy}(k)$ dashed curve upper graph, and the backwards predictive coherence function, ${}_p\gamma^2_{yx}(k)$ dashed curve lower graph, plotted in comparison with the ordinary coherence function, solid curve in both graphs, for the road noise data.*